

# Confocal Raman Imaging and Chemometric Analysis of Battery Electrode Degradation



AN\_R38: Matthew E. Berry

## Introduction

Photo-rechargeable batteries (PRBs) integrate light-harvesting and electrochemical energy storage into a single photoelectrode, enabling compact, self-powered designs for off-grid electronics, IoT devices, and sensors. The central challenge of PRBs is durability: photoelectrodes must withstand simultaneous electrochemical cycling and photoexcitation, which drives complex, poorly-understood degradation.<sup>1</sup>

Confocal Raman microscopy is ideally suited to meet this challenge. Standard electrochemical metrics, such as capacitance fade and coulombic efficiency, can flag degradation but offer no mechanistic explanation. Raman provides label-free chemical specificity, non-destructive analysis, and sub-micron spatial resolution across the full compositional range of battery electrodes: carbonaceous materials, metal oxides, and inorganic/organic electrolyte components. Coupled with chemometric analysis, it resolves individual species within complex composites and maps their spatial distribution, directly linking where degradation occurs to why it occurs.

In this Application Note, we demonstrate the Edinburgh Instruments RMS1000 Confocal Multimodal Microscope for PRB electrode analysis and mechanistically characterise a cycled  $\text{TiO}_2/\text{K}_2\text{Ti}_4\text{O}_9/\text{rGO}$  photoelectrode in a lithium-metal photo-rechargeable battery (LMPRB). Non-negative least squares (NNLS) unmixing revealed cycling-induced growth of the solid electrolyte interphase (SEI). These findings were published in *EES Batteries* and recognised as a HOT article.<sup>2</sup>

## Materials and Methods

Samples were analysed using an RMS1000 Confocal Raman microscope equipped with a 532 nm Nd:YAG laser, a 1200 l/mm diffraction grating, and a thermoelectrically cooled back-illuminated CCD camera. Fresh and cycled electrodes were mapped in 2D, and the resulting Raman imaging data were processed in the Python IDE in Ramacle<sup>®</sup> after cosmic ray removal was applied.

The photocatalytic electrodes were prepared by the TEMD Research Group at London South Bank University. They consisted of a carbon felt substrate with a  $\text{TiO}_2/\text{K}_2\text{Ti}_4\text{O}_9/\text{rGO}$  composite, incorporating both anatase and B-phase  $\text{TiO}_2$  polymorphs. A pristine, uncycled electrode and an *ex-situ* electrode (cycled 300 times at 3 V in a lithium-metal half-cell configuration with a  $\text{LiPF}_6$  and ethylene carbonate/diethyl carbonate, or EC/DEC, electrolyte) were analysed. A schematic of the cell is shown in Figure 1.

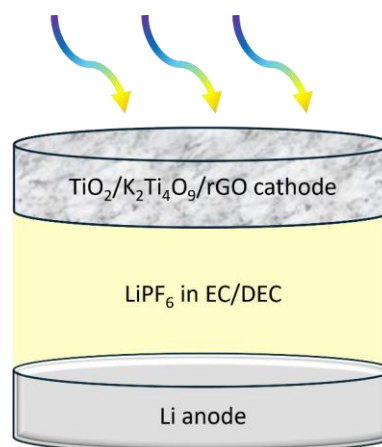


**Figure 1.** Schematic of a lithium-metal photo-rechargeable battery containing a  $\text{TiO}_2/\text{K}_2\text{Ti}_4\text{O}_9/\text{rGO}$ /carbon felt photocathode, a lithium-metal anode, and an electrolyte consisting of  $\text{LiPF}_6$  in EC/DEC.

Preprocessing prior to chemometric analysis comprised baseline correction (using a third-order polynomial), negative intensity clipping, Savitsky-Golay smoothing (with a filter window of 9 points and a third-order polynomial), and normalisation between 0 and 1. This ensured that the subsequent chemometric imaging method was performed on spectral data free of confounding baseline effects and noise.

To quantitatively resolve the contributions of components across the electrode surface, pre-processed Raman spectra were unmixed using an NNLS approach in the Ramacle Python IDE. This method assumes that each measured spectrum,  $S_i$ , can be expressed as a linear combination of a chosen number of reference spectra,  $R_j$ , weighted by their corresponding fractions,  $f_j$ , plus a residual term,  $\epsilon_i$ , representing the portion of the spectrum not explained by the model.<sup>3</sup> This is expressed in Equation 1.

$$(1) S_i \approx f_{\text{Comp } 1} R_{\text{Comp } 1} + f_{\text{Comp } 2} R_{\text{Comp } 2} + \dots + \epsilon_i, f_j \geq 0$$

Component assignment for NNLS was based on characteristic Raman bands of  $\text{TiO}_2$  anatase,  $\text{TiO}_2$  (B),  $\text{K}_2\text{Ti}_4\text{O}_9$ , rGO, and a  $\text{LiPF}_6$ -derived SEI contribution.<sup>2</sup> Reference spectra for each component were generated by averaging the spectra from the 20 pixels exhibiting the highest intensity in the preprocessed Raman maps. NNLS then solved for the non-negative fractions,  $f_j$ , for each spectrum, ensuring that the resulting values were meaningful. The fraction maps provide a quantitative spatial representation of each component, while the residuals,  $\epsilon_i$ , indicate the degree to which the linear model captures the measured spectral variation. This approach enables clear visualisation of the distribution of metal oxides and rGO coverage

# Confocal Raman Imaging and Chemometric Analysis of Battery Electrode Degradation

AN\_R38: Matthew E. Berry

across the electrode, providing mechanistic insights into degradation after cycling.

## Fresh Electrode Analysis by Confocal Raman Imaging and NNLS

The pristine, uncycled  $\text{TiO}_2/\text{K}_2\text{Ti}_4\text{O}_9/\text{rGO}$  electrode was first mapped to establish the spatial distribution of the constituent phases before electrochemical cycling. In contrast to a simpler binary oxide/carbon system, this electrode exhibits overlapping Raman contributions from anatase  $\text{TiO}_2$ ,  $\text{TiO}_2(\text{B})$ ,  $\text{K}_2\text{Ti}_4\text{O}_9$ , and rGO. Establishing this baseline is therefore essential for interpreting how the electrode evolves after prolonged cycling and for distinguishing true chemical change from spectral overlap.

Figure 2 presents the NNLS analysis for the fresh electrode. The NNLS model used enabled the contributions from anatase  $\text{TiO}_2$ ,  $\text{TiO}_2(\text{B})$ ,  $\text{K}_2\text{Ti}_4\text{O}_9$ , and rGO to be separated despite substantial spectral overlap.

This is particularly important for titanate and titania phases, whose bands can partially overlap, making direct interpretation of complex electrode spectra unreliable without chemometric separation.

The fresh-electrode NNLS analysis shows a heterogeneous but strongly integrated multiphase structure. Anatase  $\text{TiO}_2$  provides the most continuous oxide contribution across the mapped region, while  $\text{TiO}_2(\text{B})$  and  $\text{K}_2\text{Ti}_4\text{O}_9$  appear as more localised domains within the same electrode area. The rGO contribution forms an interconnected network that is consistent with its role as a conductive scaffold and interfacial support phase. Rather than indicating isolated particles, the maps are consistent with a closely coupled composite in which the active oxide and carbonaceous components are intimately distributed at the microscale.

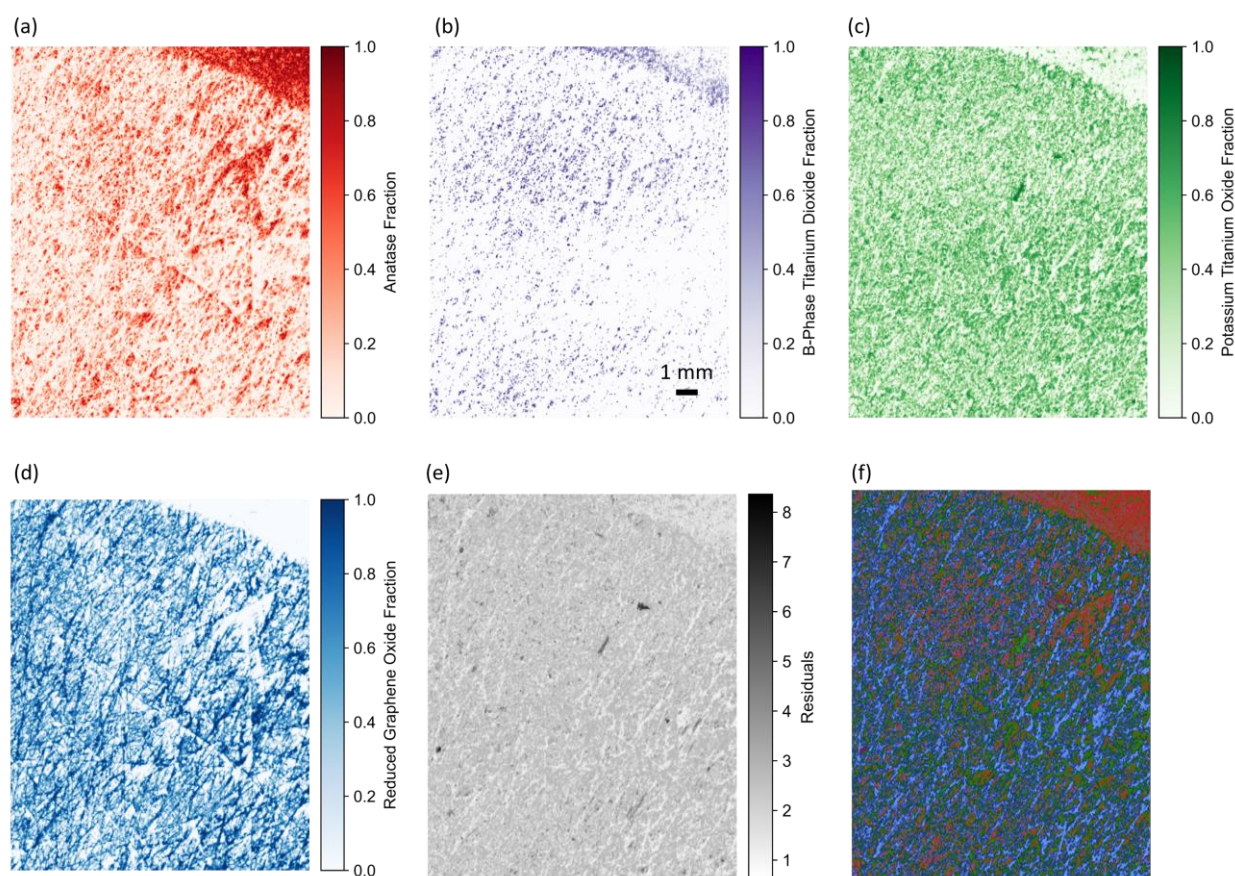


**Figure 2.** Confocal Raman and NNLS analysis of the pristine  $\text{TiO}_2/\text{K}_2\text{Ti}_4\text{O}_9/\text{rGO}$  electrode. NNLS fraction maps for (a)  $\text{TiO}_2$  anatase, (b)  $\text{TiO}_2(\text{B})$ , (c)  $\text{K}_2\text{Ti}_4\text{O}_9$ , and (d) rGO, which provide clear spatial separation of the overlapping components. (e) NNLS residual map, where low residual intensity confirms that the linear model captures the principal spectral variation across the fresh electrode surface. (f) Composite NNLS map showing the four NNLS fraction maps overlaid.

# Confocal Raman Imaging and Chemometric Analysis of Battery Electrode Degradation

AN\_R38: Matthew E. Berry

## Cycled Electrode Analysis and Evidence for SEI-Dominated Degradation

The imaging workflow was then applied to the cycled electrode to determine how the surface chemistry changed after prolonged operation. In contrast to the fresh-electrode maps, the post-cycling data show that the surface is no longer best described by the original oxide, titanate, and carbon components. Instead, the cycled electrode exhibits strong evidence of SEI formation, with its Raman contribution becoming the dominant feature in the mapped area. We therefore expanded the original NNLS model, containing anatase  $\text{TiO}_2$ ,  $\text{TiO}_2(\text{B})$ ,  $\text{K}_2\text{Ti}_4\text{O}_9$ , and rGO, to include a spectral component assigned to a  $\text{LiPF}_6$ -derived SEI-related contribution. The results of this unmixing model applied to the cycled electrode Raman map are shown in Figure 3. The persistence of the original phase signatures, alongside the emergence of a dominant SEI-related contribution, indicates that long-term degradation is governed primarily by interfacial SEI accumulation and surface masking rather than bulk active-material collapse. The higher residuals in the cycled electrode were assigned to a higher degree of

spectral complexity from the growth of the SEI-related structures on the electrode.

## Conclusions

Confocal Raman imaging, combined with chemometric analysis in the Ramacle Python IDE, has proven to be a powerful approach for the mechanistic investigation of complex lithium-metal photo-rechargeable battery electrodes. Using the RMS1000 Confocal Multimodal Microscope, we mapped pristine and cycled  $\text{TiO}_2/\text{K}_2\text{Ti}_4\text{O}_9/\text{rGO}$  electrodes with high spatial and chemical resolution, enabling the spatial distributions of anatase  $\text{TiO}_2$ ,  $\text{TiO}_2(\text{B})$ ,  $\text{K}_2\text{Ti}_4\text{O}_9$ , and rGO to be resolved despite substantial spectral overlap.

NNLS unmixing provided quantitative fraction maps that distinguish the fresh multiphase electrode architecture from the chemically evolved cycled surface. After cycling, the Raman maps become dominated by a  $\text{LiPF}_6$ -derived SEI-related contribution, while the oxide and rGO signals are attenuated rather than lost completely. This

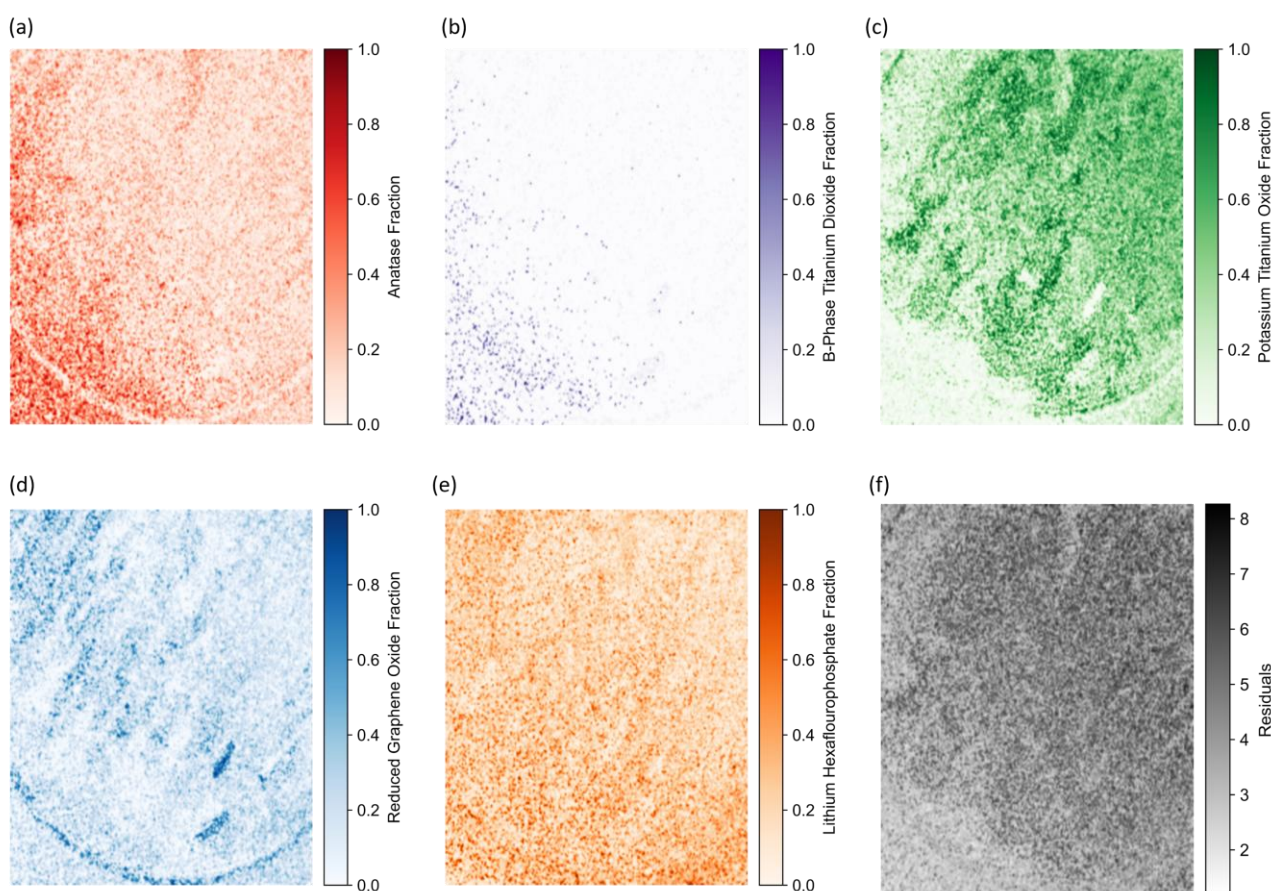


**Figure 3.** Confocal Raman and NNLS analysis of the cycled  $\text{TiO}_2/\text{K}_2\text{Ti}_4\text{O}_9/\text{rGO}$  electrode. NNLS fraction maps for (a)  $\text{TiO}_2$  anatase, (b)  $\text{TiO}_2(\text{B})$ , (c)  $\text{K}_2\text{Ti}_4\text{O}_9$ , (d) rGO, and (e)  $\text{LiPF}_6$ -derived SEI, which provide clear spatial separation of the overlapping components. (f) NNLS residual map, where low residual intensity confirms that the linear model captures the principal spectral variation across the cycled electrode surface.

# Confocal Raman Imaging and Chemometric Analysis of Battery Electrode Degradation



AN\_R38: Matthew E. Berry

---

indicates that long-term degradation is governed primarily by interfacial SEI accumulation and surface masking, rather than by selective active-phase failure or bulk structural collapse. These findings show how high-resolution, label-free Raman imaging can provide valuable mechanistic insight into electrode degradation pathways and support the development of more durable photo-assisted energy-storage materials.

## References

1. A. D. Salunke *et al.*, *ACS Appl. Energy Mater.*, 2022, **5**, 7891-7912.
2. M. Nazir *et al.*, *EES Batteries*, Advance Article.
3. Z.-M. Zhang *et al.*, *Chemom. Intell. Lab Syst.*, 2014, **137**, 10-20.

## Full Article

This work was published in *EES Batteries* in collaboration with the TEMD Research Group at London South Bank University. The full article can be found [here](#).



For more information, please contact:

+44 (0) 1506 425 300  
[sales@edinst.com](mailto:sales@edinst.com)  
[www.edinst.com](http://www.edinst.com)